EXAFS Spectroscopy with Amorphous Transition Metal-Metalloid Alloys

Friedrich Schmückle, Peter Lamparter, and Siegfried Steeb
Max-Planck-Institut für Metallforschung, Institut für Werkstoffwissenschaften, Stuttgart

Z. Naturforsch. **37 a**, 572–580 (1982); received February 16, 1982

EXAFS measurements were performed with amorphous $T_{80}M_{20}$ (T = Fe, Co, Ni; M = B, P). For the interpretation of the EXAFS spectra it was necessary also to compare them with spectra obtained from crystalline specimes with known atomic arrangement and with similar chemical composition such as the alloys Fe_2B, Co_3B, Ni_3B as well as Fe_3P, Co_3P, and Ni_3P. As a radiation source the Ag-target of a rotating anode X-ray generator (6 kW) was used. The spectra were obtained using a flat LiF-(220) monochromator. The specimens were kept at 80 K and thus thermal effects could be reduced. The EXAFS spectra of the amorphous alloys and those of the corresponding crystalline compounds of the type T_3M show among each other a relatively great similarity. The greatest similarity exists in the case of the Ni- and Co-alloys. The amorphous alloys based on iron however show larger discrepancies with respect to the corresponding crystalline ones, where the greatest deviation occurs with the compound Fe_2B. The Fourier transforms show such similarities too. The EXAFS spectra of the crystalline elements Fe, Co, and Ni as well as their Fourier transforms evidently show differences compared to the amorphous specimens and to the T_3M compounds.

The similarities observed between the amorphous alloys and the corresponding crystalline specimens of the T_3M-type together with their large discrepancies with respect to the pure metals led to the conclusion that the local structure in the amorphous alloys is in considerable accordance with that of the corresponding T_3M-compound.

Introduction

The atomic scale structure of metallic glasses has been investigated up to now most frequently by means of conventional methods such as X-ray-, electron-, and neutron-diffraction [1, 2]. In the last years, however, measurements of the fine-structure of X-ray absorption edges (EXAFS) have been used to an increasing extent for the determination of local atomic arrangements [3 – 6].

Compared with the usual diffraction methods, EXAFS has the advantage of giving information concerning the local atomic arrangement around a specific atomic species. In contrast to this, a diffraction experiment yields information of atomic arrangements around a reference atom which represents an average of all atomic species present in the specimen.

For energies larger than a characteristic threshold energy, each element shows a sudden rise of the X-ray absorption coefficient forming an edge. The appearance of this edge is related with the fact that for energies larger than this threshold energy the excitation of electrons out of an inner shell becomes possible. Phenomena related with this edge therefore allow to make statements concerning the specific atomic species.

In an EXAFS experiment, the quantity of interest is the modulation $\chi(k)$ of the X-ray absorption coefficient in the energy range just above an absorption edge, in the present case the K-absorption edge of the metallic alloy components Fe, Co or Ni. This modulation extends over an energy range of several hundred electron volts above the absorption edge.

According to present ideas, the appearance of this modulation is due to local interference effects of the photoelectrons produced during the absorption process. Such a photoelectron travels as a wave away from the atom ionized during the absorption process and it can be backscattered to the original atom by neighbouring atoms. The modulations observed in the X-ray absorption coefficient can be explained as an interference between the outgoing and the backscattered wave [7 – 10].

In reverse, following the analysis of this modulation one can draw conclusions concerning the local atomic arrangement in the environment of the atomic species under consideration [11 – 14].

Theory

The quantum mechanical treatment of the photoabsorption within the limit of the dipole-approxima-

Reprint requests to Prof. Dr. S. Steeb, NPI-Metallforschung, Institut für Werkstoffwissenschaften, Seestr. 92 7 Stuttgart 1, Germany.

0340-4811 / 82 / 0600-0572 $ 01.30/0. — Please order a reprint rather than making your own copy.

tion and with restriction to single-scattering yields as expression for the EXAFS modulation of a multicomponent system above the K-edge of α-type atoms [14, 15]:

$$\chi_\alpha(k) = -\frac{1}{k}\sum_\beta \int_0^\infty \mathrm{d}r \frac{G_{\alpha\beta}(r)}{r^2} D(r) \cdot \Im\mathrm{m}\{f_\beta(k,\pi) e^{2i(kr+\delta_\alpha(k))}\}. \quad (1)$$

$G_{\alpha\beta}(r)$ are the partial radial atomic distribution functions. Loss mechanisms such as inelastic scattering or relaxation effects cause an amplitude damping of $\chi(k)$ and are taken into account by the damping factor $D(r)$ [16]. These loss mechanisms form the reason, why in practice only the nearest neighbours give a contribution to the EXAFS modulation. Therefore EXAFS measurements are especially convenient to yield informations concerning local atomic scale structures. $f_\beta(k,\pi)$ is the backscattering amplitude of electrons from β-type atoms. $\delta_\alpha(k)$ describes the photoelectron phaseshift in the core-region of an α-type atom ionized by photoabsorption.

With the Fourier transform

$$F(r) = \frac{1}{\sqrt{2\pi}} \int_0^\infty \mathrm{d}(2k) e^{-2ikr}(-k\chi) \quad (2)$$

and with Eq. (1) one obtains the function:

$$F_\alpha(r) = \sum_\beta \int_0^\infty \frac{G_{\alpha\beta}(r') D(r')}{r'^2} \xi_{\alpha\beta}(r-r')\,\mathrm{d}r', \quad (3)$$

where

$$\xi_{\alpha\beta}(r) = \frac{1}{2i\sqrt{2\pi}} \cdot \int_0^\infty \{f_\beta(k,\pi) e^{2i\delta_\alpha(k)}\} e^{-2ikr}\,\mathrm{d}(2k).$$

Therefore $\xi_{\alpha\beta}$ is the Fourier transform of the scattering amplitude. Caused by the k-dependence of the phase shift $\delta_\alpha(k)$, the peak of $|\xi_{\alpha\beta}|$ is not located at $r=0$ in general, but is shifted to a negative r-value. Therefore, the peaks in $|F_\alpha(r)|$ are shifted by the same extent with respect to the true atomic distances. The damping factor $D(r)$ reaches zero as the distance exceeds the nearest neighbour distance so that the evaluation of EXAFS spectra has to be restricted in general to the first coordination shell. Another important fact is that the experimental data are restricted in k-space, typically between $k=3$ Å^{-1} and $k=12$ Å^{-1} in the case of the metallic glasses, so that the peaks in r-space are additionally broadened. Therefore, the peak width in r-space is not a direct measure for the spread of distance values in the atomic distribution [17]. A commonly used method in EXAFS investigations is the back-transform to k-space of only that peak in $F(r)$ which corresponds to the first coordination shell. Introducing for the description of the first coordination shell a function $S_1(r-R_1)$, which has a peak at the mean atomic distance R_1 and is located between $r=r_1$ and $r=r_2$, one obtains using the back-transform

$$\chi_1(k) = -\frac{1}{k}\int_{r_1}^{r_2} F(r) e^{2ikr}\,\mathrm{d}r \quad (4)$$

the following expression:

$$\chi_{\alpha,1} = -\frac{D_1}{k R_1^2} \cdot \Im\mathrm{m}\{s_1(k) f_1(k,\pi) e^{2i(\delta_\alpha(k)+kR_1)}\} = -\frac{D_1}{k R_1^2} |s_1(k)||f_1(k,\pi)| \cdot \sin(2kR_1 + \varphi_1(k)), \quad (5)$$

where

$$\varphi_1(k) = 2\delta_\alpha(k) + \arg(f_1(k,\pi)) + \arg(s_1(k)).$$

It is seen that $s_1(k)$ is the Fourier transform of $S_1(r)$. For simple systems, S_1 can be assumed to be a Gaussian with width σ_1:

$$S_1(r-R_1) = \frac{N_1}{\sqrt{2\pi}\sigma_1} \cdot \exp\left\{-\frac{1}{2}\left(\frac{r-R_1}{\sigma_1}\right)^2\right\}. \quad (6)$$

The corresponding expression for $s_1(k)$ is:

$$s_1(k) = N_1 e^{-2\sigma_1^2 k^2}, \quad (7)$$

where N_1 is the coordination number of the first shell. In this special case of a symmetric atomic distribution $\arg(s_1(k))$ is equal to zero.

In the case of strongly disordered systems such as the metallic glasses this description with a Gaussian is no good approximation and an asymmetric distribution around R_1 has to be expected [4, 17]. But in this case $\arg(s_1(k)) \neq 0$, so that an additional phase shift appears. For this reason, a direct evaluation of EXAFS spectra starting from (Eq. (3) to Eq. (7) without additional assumptions seems impossible for strongly disordered systems. For this case it is most suitable to perform reference-measurements with specimens with known crystallographic structure whose chemical composition is near to the

composition of the unknown substances. For the metallic glasses of the type $T_{80}M_{20}$ investigated during the present work, these are the stable crystalline phases of the T_3M-type, the crystallographic data of which are known rather exactly in most cases.

Experimental Procedure

Sample Preparation

The metallic glasses have been prepared by the meltspinning method as long ribbons approximately 1 – 2 mm wide and 30 μm thick. The samples were 20 mm long sections out of such ribbons, which have been thinned to the required thickness of about 10 μm by means of a combination of mechanical grinding and electrochemical polishing. The samples for the reference measurements with the crystalline alloys of the T_3M-type were grinded to a fine powder in a ball mill. Subsequently the powder was annealed for two hours at approximately 600 °C. For the measurements the powder was prepared as a thin layer onto Tesa-Film and care was taken to achieve a uniform distribution of the powder on the supporting foil.

Measurements

During the measurements the samples were mounted in a liquid nitrogen cryostat and held at a temperature of 80 K. As radiation source, a rotating anode X-ray generator with an Ag-Target and with a maximum power of 6 kW was used. A flat LiF-(220) crystal was used for the spectral analysis of the radiation. Dependent on its angular position, this crystal selects out of the incident radiation a fixed wavelength λ, according to Bragg's relation.

Monochromatic radiation could be provided therefore by variation of the angle θ. The spectral resolution $\Delta\lambda/\lambda$ had a value of about $1.4 \cdot 10^{-3}$, which could be tested by measuring the width of the WL_{α_1}-line. The EXAFS spectra were recorded by scanning the angle θ in steps of $\Delta\theta = 0.01°$. At each data point the transmitted intensity I as well as the incident intensity I_0 were measured, the latter by pulling the sample out of the beam by means of a special setup installed in the cryostat. Therefore, possible long-periodic intensity fluctuations of the radiation source could be compensated. To achieve good statistical accuracy, 10^6 counts were preselected for each data point. The data processing was done using a PDP 11/34 computer.

Spectra Normalization

The calibration of the energy-scale was done using the emission lines of some characteristic contaminations (Cu, W, Zn) which were always present on the Ag-target.

The subtraction of the background not resulting from K-absorption processes was done in the usual manner by fitting with a Victoreen formula. A problem with EXAFS measurements is the exact definition of the zero point E_0 for the kinetic energy of the photoelectrons, which is: $E_{kin} = h\nu - E_0$, where $h\nu$ is the energy of the incident X-ray quanta. In other papers [15, 18, 19] people often tried to avoid this difficulty by treating E_0 as a variable fitting parameter. For comparing the results of several runs done with different samples, in the present paper a different procedure has turned out to be more suitable: At the half-height of the absorption edge, which rises within an energy region of 15 – 20 eV, the tangent is drawn. It intersects the abscissa at a point which defines the zero point of energy. Thus one has a procedure consistent for all measurements. Possible deviations from the true value of E_0 therefore appear in a uniform way in all measurements and so no problems arise when the measurements are compared among each other.

The extraction of the EXAFS modulation $\chi(k)$ was done in the usual way by fitting a polynomial to the measured spectra in the energy region above the absorption edge. Polynomials with 4th to 6th degree have turned out to be optimal for this purpose. By this procedure the "base line" of the spectra was obtained, which finally is represented by the zero line of the EXAFS spectra as presented for example in Figure 1 a.

The EXAFS modulation is superposed as a weak signal on a very high background. Therefore, the function $\chi(k)$ has much more noise than the total spectrum measured with a statistical accuracy of 0.2%. Thus a smoothing procedure was necessary before further interpretation of the data. The smoothing was done with a "cubic spline-fit" algorithm, which approximated the data sectionally by polynomials of 3rd degree. The function obtained in this way was the starting point for all the interpretations performed further.

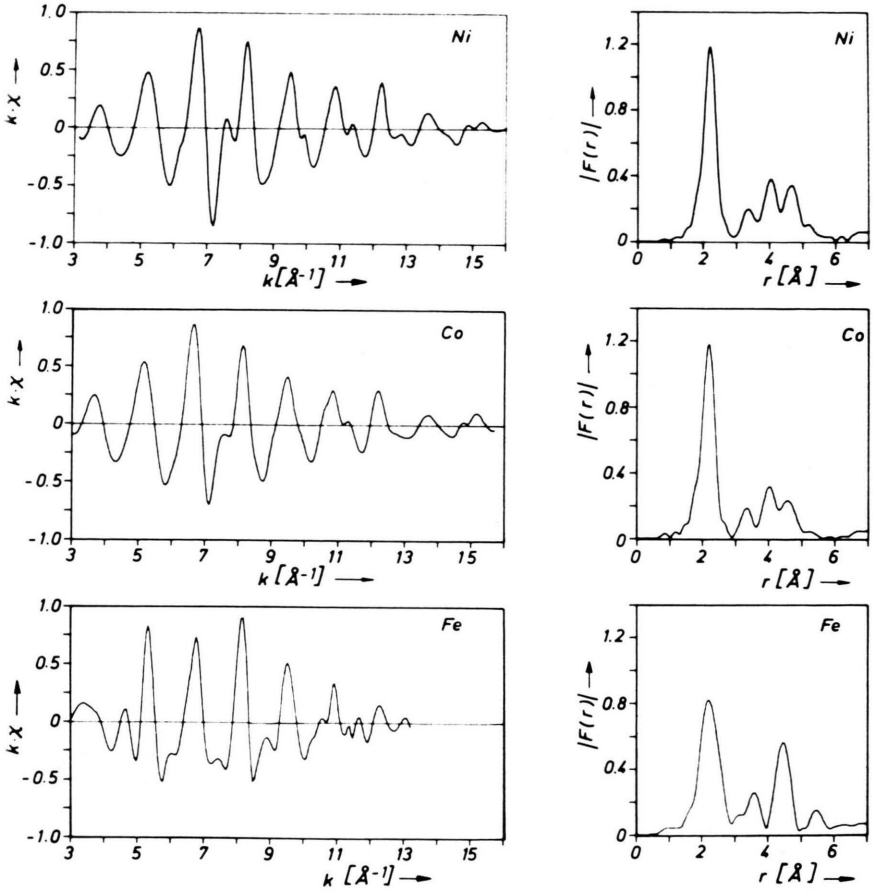

Fig. 1. Crystalline elements Fe, Co, and Ni: EXAFS spectra and their Fourier transforms (measured at $T = 80$ K). a) EXAFS spectra $k \cdot \chi$; b) Magnitude of the Fourier transform $|F(r)|$.

Results and Discussion

EXAFS Spectra

In Fig. 1 the EXAFS spectra measured with the crystalline elements Fe, Co, and Ni and their Fourier transforms are shown. In Figs. 2 and 3 the spectra of the amorphous B- and P-alloys are compared with those of the corresponding crystalline phases.

The EXAFS spectra of the amorphous B- and P-alloys in Figs. 2 and 3 all have a very similar shape. They consist of a damped oscillation with a relatively uniform frequency. The absence of higher-frequency portions in these spectra is due to the absence of strong correlations between the central atom and the more distant neighbours in the amorphous state.

One can get more information comparing the EXAFS spectra measured with the amorphous alloys and those of the crystalline elements Fe, Co, and Ni (Fig. 1) as well as those of the corresponding crystalline B- and P-alloys (Figures 2 b and 3 b). Here one can recognize in some cases a large similarity between the spectra of the amorphous alloys and those of the corresponding crystalline compounds. Especially the amplitude of the EXAFS modulation has a comparable magnitude in these cases, whereas for the pure elements (Fig. 1) the magnitude is greater by a factor 3 – 4. Altogether, the spectra of the crystalline TM-alloys show a more detailed structure, which indicate larger long range order compared with the case of the amorphous alloys, because as already mentioned above, the higher-frequency components in the EXAFS spectrum are caused by the contributions of the more distant neighbouring atoms.

The best correspondence between the amorphous alloys and the crystalline compounds is found in the

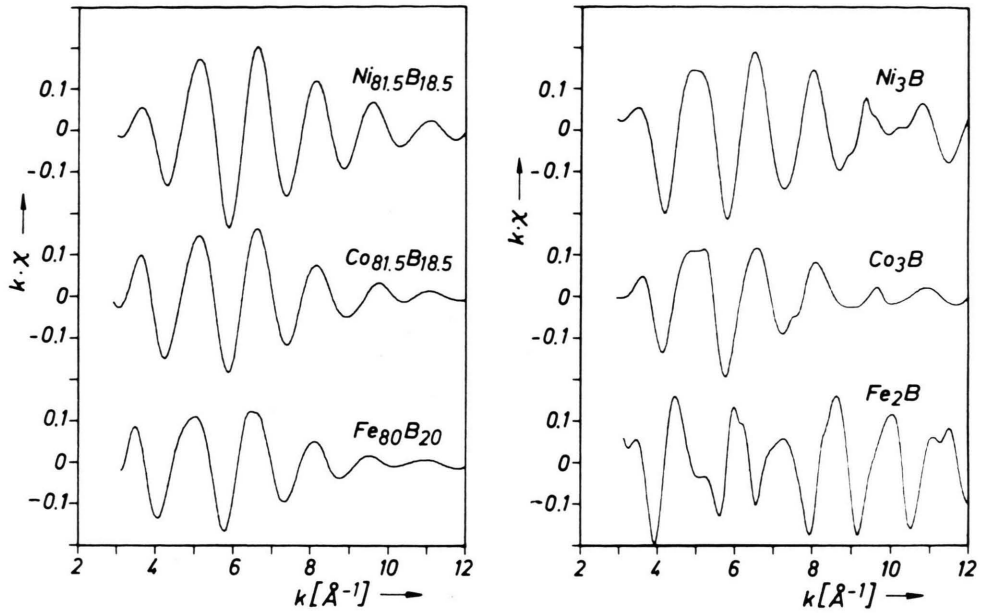

Fig. 2. EXAFS spectra of amorphous and crystalline transitionmetal-boron alloys. a) amorphous alloys; b) crystalline compounds.

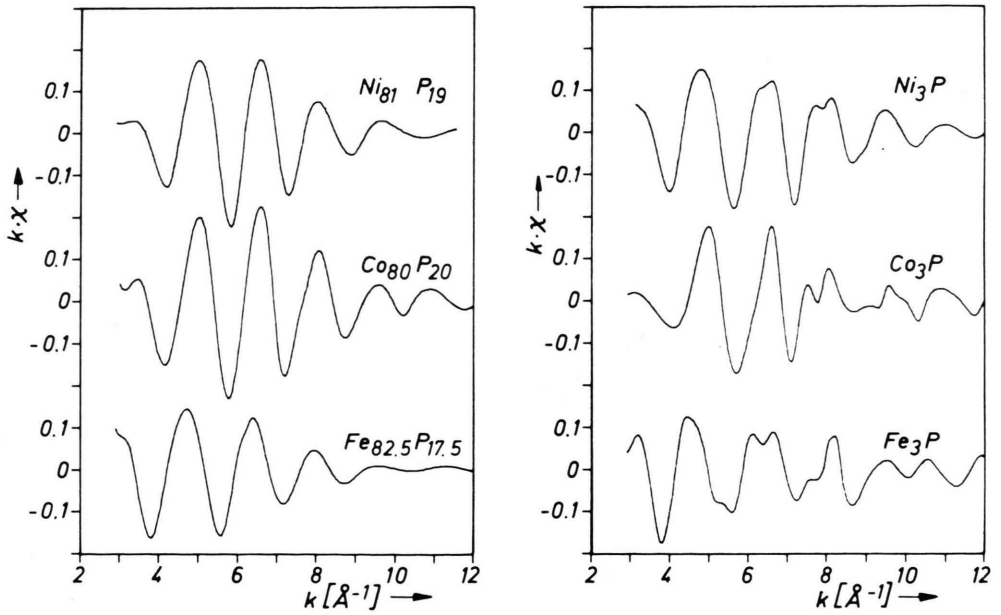

Fig. 3. EXAFS spectra of amorphous and crystalline transitionmetal-phosphorous alloys. a) amorphous alloys; b) crystalline compounds.

case of the Ni-alloys. With the Co-alloys, the correspondence is relatively good too, whereas the greatest differences occur with the Fe-alloys. Especially the composition Fe_2B shows the largest diviations, which can be related to the fact that in this case the metalloid concentration also shows the largest difference and therefore, with respect to the chemical point of view there is also the smallest relation between the crystalline reference substance and the amorphous alloy. This example shows clearly, that for EXAFS investigations it is very important to use for the purpose of reference measurements only such

crystalline substances which are chemically very close related to the unknown system.

The fact, that the amplitude of the EXAFS modulation in the amorphous and in the crystalline TM-alloys is in both cases reduced by the same factor in comparison with the spectrum of the corresponding pure element indicates that the nearest-neighbour distances in these systems show a larger spread than in the case of the pure elements and that the mean distances R_1 have approximately the same value. Some exceptions from this conclusion is formed by the compound Fe_2B in the case of the iron-alloys. By comparing the EXAFS spectra it can be derived therefore, that the arrangement of nearest neighbours in the amorphous systems and in the corresponding crystalline T_3M-compounds shows a certain degree of similarity.

At this point the paper [20] should be mentioned, where the EXAFS spectrum of amorphous $Co_{76}P_{24}$ (produced by electrochemical deposition) is compared with the spectra of crystalline Fe_3P, Fe_2P, and Co_2P. The comparison with the spectra obtained during the present paper shows especially in the case of the crystalline substances a more smooth run and much lower amplitudes in [20]. This probably can be ascribed to the higher sample temperatures which were applied in [20].

Fourier Transforms

As well as the EXAFS spectra of the amorphous B- and P-alloys also their Fourier transforms presented in Fig. 4 and Fig. 5 show relatively large similarities. In the case of the Ni- and Co-systems their striking relationship to the corresponding crystalline T_3M-compounds is to be mentioned, too. The largest differences again occur in the case of the Fe-alloys. Especially with the compound Fe_2B the first peak in $|F(r)|$ is clearly split into two subpeaks.

As in the case of the crystalline elements Fe, Co, and Ni in Fig. 1 the peaks corresponding to the first coordination shell in Fig. 4 and Fig. 5 yield the dominating contribution to $|F(r)|$. Compared with the amorphous alloys, the crystalline TM-alloys clearly yield more contributions from more distant coordination shells which however are much less pronounced than in the case of the pure elements.

The metal-metal distances as well as the metal-metalloid distances give contributions to the first peak of the Fourier transforms. The difference between these distances, however, is not spatially resolved in $|F(r)|$. The main reason for this is expected to be the relatively low scattering power of the metalloid atoms compared to that of the metal atoms. The shoulders occuring in some cases at the front side of the first peak in the region of 0.8 Å – 1.2 Å must not be regarded as metal-metalloid distances, as their shape depends strongly on the polynomial degree chosen for the normalization of the spectra. Therefore they have no real physical meaning.

In the case of the amorphous transition metal-boron alloys, the second peak in $|F(r)|$ is split into two subpeaks. This effect is most obvious for amorphous $Fe_{80}B_{20}$, whereas the splitting with $Co_{81.5}B_{18.5}$ and $Ni_{81.5}B_{18.5}$ is less pronounced. The amorphous transition metal-phosphorous alloys however show much more smeared out structures beyond the first coordination shell.

Such splitting of the second peak in $|F(r)|$ have been found by other authors with EXAFS investigations on amorphous alloys of the type $Fe_{40}Ni_{40}B_{20-x}P_x$ (with $x=0-20$) [5, 6]. Also X-ray diffraction experiments with the amorphous alloys $Co_{81.5}B_{18.5}$ and $Fe_{80}B_{20}$ in [2] yielded a strongly split second peak in the reduced pair-distribution function $G(r)$.

In the case of the crystalline TM-compounds, the Fourier transforms $F(r)$ exhibit beyond the first coordination shell a greater magnitude and a longer extension in r-space than the corresponding amorphous alloys. This can be attributed to the more pronounced long-range order in these systems. However, the r-dependence of these parts of the curves shows no uniform tendency in the T-B- as well as in the T-P-series and is strongly smeared out in some cases although the underlying crystal structures are very similar. These differences are at least partly due to non-ideal sample geometry because with the crystalline TM-compounds it was not possible to avoid completely some inhomogeneities in the layer of the powdered sample substances during the coverage of the supporting foils.

Atomic Distances

For the determination of atomic distances it has to be considered, that the positions of the maxima in $|F(r)|$ do not correspond to the true atomic dis-

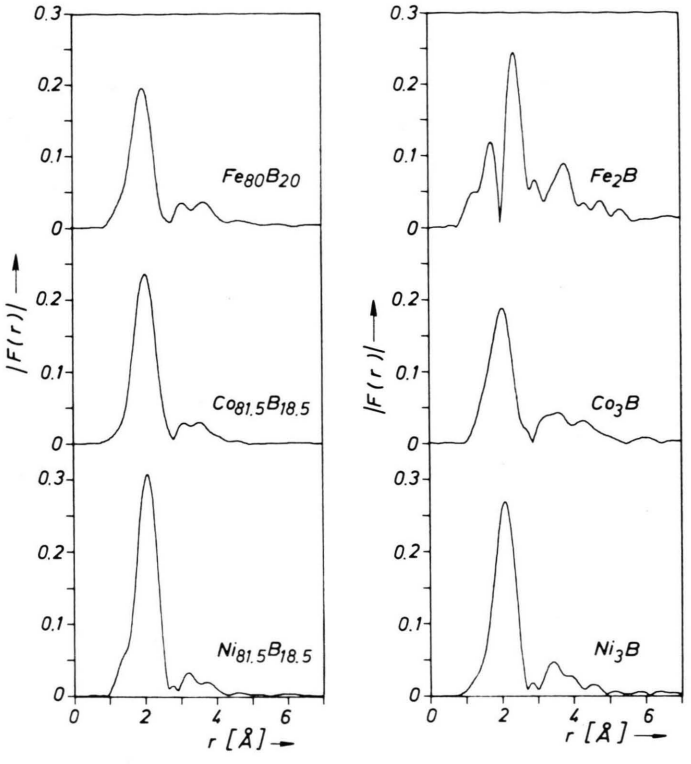

Fig. 4. Magnitude of the Fourier transform of the EXAFS spectra of amorphous and crystalline transitionmetal-boron alloys. a) amorphous alloys; b) crystalline compounds.

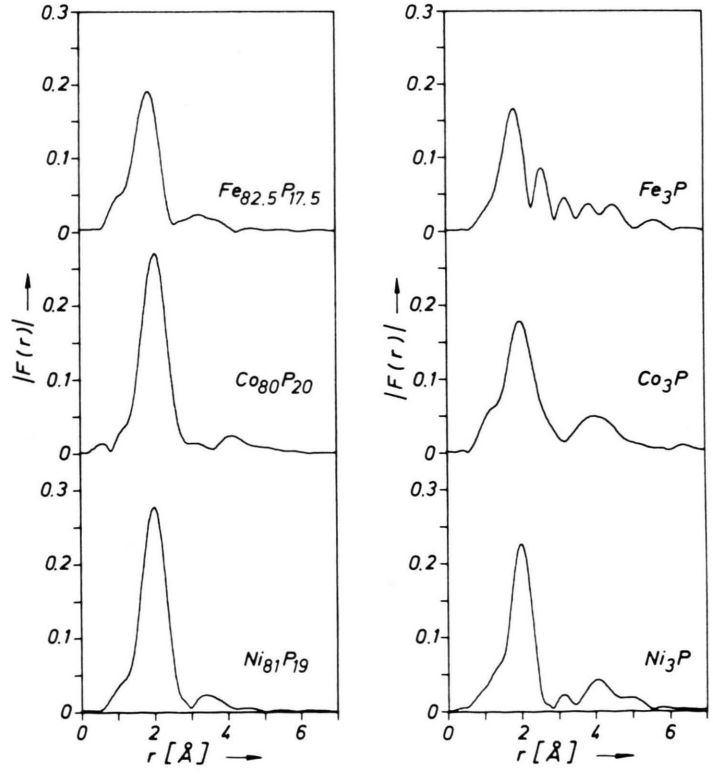

Fig. 5. Magnitude of the Fourier transform of the EXAFS spectra of amorphous and crystalline transitionmetal-phosphorous alloys. a) amorphous alloys; b) crystalline compounds.

tances but that they are shifted to smaller r-values because of the k-dependence of the phase-shift $\varphi(k)$. To determine $\varphi(k)$ experimentally using Eq. (5) by performing a reference measurement with a suitable substance it is necessary to know R_1 of the reference substance. This is connected to the condition that the radial atomic distribution within a coordination-shell can be well described by a Gaussian. However, this condition is not fulfilled by the T_3M-compounds which have a relatively complicated crystal structure, because it turns out for example that in proximated by a linear expression of the form:

Ni_3B there exist many Ni-Ni distances between 2.43 Å and 2.79 Å which all contribute to the first peak in $|F(r)|$.

Therefore it seems more reasonable instead of trying to do an absolute determination of the atomic distances to compare the relative positions of the peaks in $|F(r)|$ for the amorphous alloys with those of the corresponding reference substances in order to obtain informations concerning possible displacements of atomic distances. During this evaluation the fact is used, that the phase-shifts can be well ap-

$$\varphi(k) = a_0 + a_1 2k. \tag{8}$$

At least for chemically closely related systems one can assume with the concept of phase-transferability [21] that their phase-shift has the same k-dependence. Equation (5) yields

$$\arg(k\chi_1) = 2kR_1 + \varphi(k). \tag{9}$$

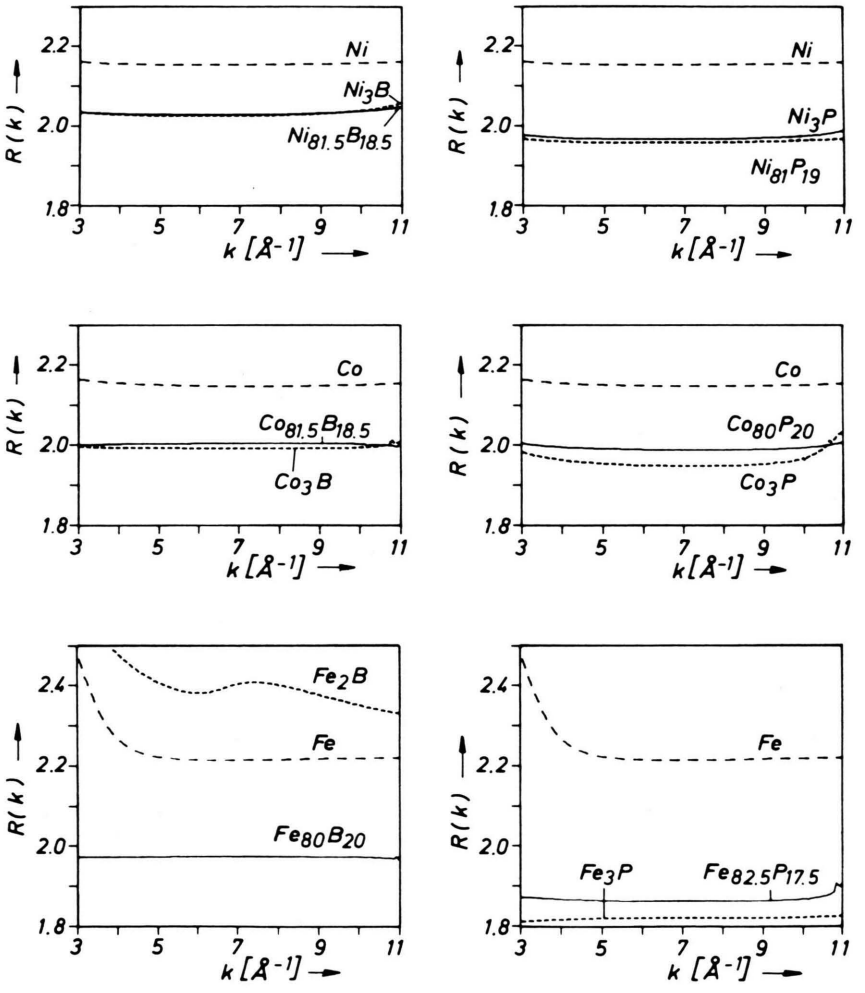

Fig. 6. $R(k)$-curves according to Eq. (10) for some T-M-alloys and the elements Fe, Co, and Ni. ----- = pure metal; ..... = crystalline T-M-alloys; ——— = amorphous alloys.

Assuming a linear expression for $\varphi(k)$ one can evaluate a function $R(k)$ which can be used for a quantitative comparison of different measurements [22]:

$$R(k) = \frac{1}{2k}(\arg(k\chi_1) - a_0). \qquad (10)$$

In each case the constant a_0 is determined by fitting a straight line to $\arg(k\chi_1)$. As the coefficients a_1 in Eq. (8) can be assumed to have the same value for systems whose chemical composition and shape of the nearest neighbour distribution are similar, the $R(k)$-curves of such systems will be shifted by the same value a_1 with respect to the true distances R_1. The corresponding curves for the amorphous and for the crystalline TM-alloys as well as for Fe, Co, and Ni are shown in Figure 6.

The comparison of the $R(k)$-curves of the pure metals with those of the corresponding crystalline T_3M-compounds shows that the observed displacements are not in accordance with those expected from the known crystallographic data. For example, according to the structural data given in [23] and [24] the average Ni-Ni-distance in Ni_3B or Ni_3P is increased by 0.09 Å or 0.01 Å, respectively, in comparison with pure Ni. In contrast to this, the observed displacements of the $R(k)$-curves against Ni have values of -0.12 Å and -0.17 Å, respectively. From the crystallographic data of the T_3M-systems it is known that their nearest neighbour distributions are not symmetric, therefore a contribution from the term $\arg(s_1(k))$ in (5) to the total phase shift has to be expected [17]. However, the large shifts observed in Fig. 6 cannot be explained only as resulting from the asymmetric shape of the corresponding distribution functions. It is more likely that the difference in the type of chemical bonding in the pure metals with respect to the crystalline systems T_3M and the amorphous TM-alloys also contributes to the observed shift.

This shows clearly, that the concept of phase-shift transferability has to be used with caution and should be applied only to compare chemically closely related systems. This can be done in the case of the crystalline systems T_3M and their corresponding amorphous alloys. The fact, that the shape of the $R(k)$-curves in these cases shows a high degree of accordance, indicates that the shape of the nearest neighbour distribution is also very similar.

For example, in the case of the Ni- and Co-alloys, the differences are not greater than 0.04 Å. The Fe-P alloys also have differences of the same order of magnitude, whereas the compound Fe_2B shows a large displacement compared to $Fe_{80}B_{20}$. This corresponds to the large differences which in this case are also present in the EXAFS spectra and the Fourier transforms.

Acknowledgement

Thanks are due to the Deutsche Forschungsgemeinschaft for financial support of this work.

[1] E. Nold, P. Lamparter, H. Olbrich G. Rainer-Harbach, and S. Steeb, Z. Naturforsch. **36**a, 1032 (1981)
[2] P. Lamparter, E. Nold, G. Rainer-Harbach, E. Grallath, and S. Steeb, Z. Naturforsch. **36 a**, 165 (1981).
[3] D. Raoux, et al., Revue Phys. Appl. **15**, 1079 (1980).
[4] A. Werner, Doctor thesis, Universität Kiel 1979.
[5] J. Wong, F. W. Lytle, R. B. Greegor, H. H. Liebermann, J. L. Walter, and F. E. Luborsky, General Electric Technical Information Series, Rep. No. 78CRD253, Feb. 1979.
[6] M. de Crescenzi, A. Balzarotti, F. Comin, L. Inoccia, S. Mobilio, and D. Bacci, Fourth International Conference on Liquid and Amorphous Metals, Grenoble 1980, C8–238.
[7] D. E. Sayers, F. W. Lytle, and E. A. Stern, Adv. X-Ray Anal. **13**, 248 (1970).
[8] E. A. Stern, Phys. Rev. B **10**, 3027 (1974).
[9] P. A. Lee and J. B. Pendry, Phys. Rev. B **11**, 2795 (1975).
[10] C. A. Ashley and S. Doniach, Phys. Rev. B **11**, 1279 (1975).
[11] D. E. Sayers, E. A. Stern, and F. W. Lytle, Phys. Rev. Lett. **27**, 1204 (1971).
[12] F. W. Lytle, D. E. Sayers, and E. A. Stern, Phys. Rev. B **11**, 4825 (1975).
[13] E. A. Stern, D. E. Sayers, and F. W. Lytle, Phys, Rev. B **11**, 4836 (1975).
[14] T. M. Hayes, P. N. Sen, and S. H. Hunter, J. Phys. C **9**, 4375 (1976).
[15] P. Rabe and R. Haensel, Festkörperprobleme XX, Verlag Vieweg, Braunschweig 1980, p. 43.
[16] B. Lengeler and P. Eisenberger, Phys. Rev. B **21**, 4507 (1980).
[17] P. Eisenberger and G. S. Brown, Solid State Commun. **29**, 481 (1979).
[18] G. Martens, P. Rabe, N. Schwentner, and A. Werner, Phys. Rev. B **17**, 1481 (1978).
[19] A. Fontaine, P. Lagarde, A. Naudon, D. Raoux, and D. Spanjaard, Phil. Mag. B **40**, 17 (1979)
[20] G. S. Cargill III, Conference proceedings of the 4th Int. Conference on Rapidly Quenched Metals, held at Sendai, Japan, August 1981.
[21] P. H. Citrin, P. Eisenberger, and B. M. Kincaid, Phys. Rev. Lett. **36**, 1346 (1976).
[22] F. Schmückle, Doctor thesis, Universität Stuttgart, 1981.
[23] W. B. Pearson, Handbook of Lattice Spacings and Structures of Metals, Pergamon Press, Oxford, Vol. **1**, (1958), Vol. **2**, (1967).
[24] R. W. G. Wyckoff, Crystals Structures, 2nd Ed., Vol. **2**, Intersience, New York 1963, p. 114.